Hindawi
Andrologia
Volume 2023, Article ID 2966391, 12 pages
https://doi.org/10.1155/2023/2966391

Research Article

Androgen Receptor (AR) Depletion Underlies the Reproductive Dysfunctions in Male Rats Exposed to Alcohol and Combination Antiretroviral Therapy (cART)

Elna Owembabazi,[1,2] **Pilani Nkomozepi**,[3] **and Ejikeme F. Mbajiorgu**[1]

[1]*School of Anatomical Sciences, University of the Witwatersrand, 2193 Johannesburg, South Africa*
[2]*Department of Human Anatomy, Kampala International University, Western Campus, 71, Uganda*
[3]*Department of Human Anatomy and Physiology, University of Johannesburg, 2028 Johannesburg, South Africa*

Correspondence should be addressed to Elna Owembabazi; 2278202@students.wits.ac.za

Received 31 January 2023; Revised 23 March 2023; Accepted 31 March 2023; Published 14 April 2023

Academic Editor: Debarshi Sarkar

Copyright © 2023 Elna Owembabazi et al. This is an open access article distributed under the Creative Commons Attribution License, which permits unrestricted use, distribution, and reproduction in any medium, provided the original work is properly cited.

The prevalence of alcohol abuse and HIV/AIDS is high in males of reproductive age; unfortunately, a high incidence of alcohol intake has been reported in HIV/AIDS patients including those on combination antiretroviral therapy (cART). Incidentally, alcohol and cART use have each been implicated in male reproductive dysfunction. Therefore, the interactive effects of alcohol and cART on reproductive hormone levels, testicular connective tissue, and androgen receptor and Ki-67 expression were evaluated in HIV naïve adult male Sprague Dawley rats. Adult male rats were divided into four groups: control, alcohol (A), cART, and A+cART. Animals were terminated after 90 days of treatment; then, the blood and testis were extracted for analysis. Special staining for testicular connective tissue, immunoassay for reproductive hormones, and immunohistochemistry for androgen receptor and Ki-67 were conducted. The study found significantly ($p < 0.05$) increased thickness of seminiferous tubule basement membrane in the cART group and testicular capsule in the A+cART group. Collagen, reticulin, and elastin fibers decreased significantly in all the treated groups, except for reticulin in the testis of A group animals. With exception of luteinizing hormone in the cART group, all the treated groups had significantly elevated levels of luteinizing and follicle-stimulating hormones, but no significant ($p > 0.05$) difference was found in their testosterone and inhibin B levels. The number of Sertoli and Leydig cells expressing androgen receptor reduced significantly in all the treated groups, except for A group's number of Sertoli cells expressing androgen receptor. Further, in all the treated groups, Ki-67 expression significantly reduced relative to control. In this study, with exception of seminiferous tubule basement membrane, all study parameters were greatly altered in the A+cART group; we suggest that the exacerbated androgen receptor depletion recorded in the A+cART group might have led to the observed severe testicular structural alteration and spermatogenesis derangement.

1. Introduction

The high prevalence of combination antiretroviral therapy (cART) use [1] and alcohol abuse [2] in males of reproductive age has raised clinical concerns for male infertility. The sub-Saharan Africa region is the world's epicenter of HIV/AIDs, with a daunting prevalence consistently reported in South Africa [3]. About 20% of the adult population is living with HIV in South Africa, and thus, the use of cART is common [4]. Incidentally, the prevalence of alcohol abuse in people living with HIV/AIDS is alarming [5] and is reported to be more than twofold higher compared to that of the general populace [6], which points to both drugs being concomitantly present in the body. Moreover, alcohol and cART have each been shown to negatively impact the male reproduction system [7, 8].

Clinical studies have documented hypogonadism and feminization in male chronic alcoholics [9] and in people living with HIV/AIDS on a cART regimen [10]. The most common encountered manifestations of male hypogonadism include low testosterone levels, gonadal atrophy,

gynecomastia, and muscle wasting [10, 11]. However, hypogonadism symptoms may not be directly linked to hypothalamic-pituitary-gonadal (HPG) axis impairment but could also result from disturbances of hormone-receptor interaction and/or partial or complete receptor insensitivity [12]. Importantly, testosterone, an androgen synthesized by the Leydig cells, is essential for successful spermatozoa production (spermatogenesis) [13, 14]. The impact of testosterone is mediated via the androgen receptor [15, 16], but testosterone is also involved in the regulation of androgen receptor expression [14, 17, 18].

In the testis, androgen receptor is expressed in the nuclei of somatic cells, viz., Leydig, Sertoli, myoid, and pericyte cells [13, 19, 20], and androgen receptor has been shown to regulate the structure and functions of these cells [14, 17, 18]. Sertoli cells' androgen receptor transduces the action of testosterone on spermatogenesis because germ cells do not express androgen receptor [14, 16]. Additionally, the expression of androgen receptor by Sertoli cells is an indicator of the cells' maturity and is essential for formation of an effective blood-testis barrier that creates an immune-privileged microenvironment necessary for successful spermatogenesis [15, 16, 21]. Further, the myoid cells' androgen receptor expression is required for retinol processing, an essential factor for initiating spermatogonia differentiation [16, 18].

Thus, adequate reproductive hormone levels and hormone-receptor interactions are necessary for sufficient germ cell proliferation, differentiation, and maturation [22] and maintenance of testicular structural integrity [17, 18]. Accordingly, the current study investigated the testicular impact of alcohol and cART copresence in the body on serum reproductive hormone levels, morphometry of testicular capsule, interstitial connective tissue fibers, seminiferous tubule basement membrane, and testicular androgen receptors and Ki-67 expressions in male Sprague Dawley rats.

2. Methods and Material

2.1. Chemical and Reagents. Atripla, a fixed-dose combination antiretroviral (cART) drug, was purchased from Bristol-Myers Squibb and Gilead Sciences (Foster City, CA, USA), and androgen receptor rabbit monoclonal (ab105225) and Ki-67 rabbit polyclonal (ab15580) primary antibodies were purchased from Abcam (Cambridge, MA, USA). Then, biotinylated goat anti-rabbit (BA-1000) secondary antibody and avidin-biotin complex kit (PK-6100) were purchased from Vector Laboratories (Burlingame, CA, USA). The ELISA kits for luteinizing hormone (LH) (E-EL-R0026), follicle-stimulating hormone (FSH) (E-EL-R0391), testosterone (TT) (E-EL-R0155), and inhibin B (E-EL-R1027) were purchased from Elabscience (Houston, Texas, USA).

2.2. Ethical Clearance. The Animal Research Ethics Committee (AREC) of University of the Witwatersrand (Wits) approved the animal study protocol with approval number 2018/011/58/C. All experiments were carried out at Wits Animal Research Facility in accordance with the guidelines of AREC.

2.3. Animals. Twenty-four (24) adult male Sprague Dawley rats (10 weeks old) weighing between 330 and 370 grams were used. Since treatments were administered in drinking water (alcohol) and in gelatine cubes (cART), the rats were kept individually to ensure that each rat received the appropriate treatment dosage. The rats were housed in sterile plastic cage with pinewood shaving beddings at a room temperature of 21-23°C, with a 12-/12-hour light/dark cycle, and supplied with standard rat chow and water *ad libitum*.

2.4. Experimental Design. The animals were divided into four groups, each with six rats: control group, which received no treatment; alcohol group (A), which received daily treatment of 10% *v*/*v* alcohol in drinking water [23]; cART group, which received an animal dose adjusted from the human cART dose of 23 mg/kg daily in gelatin cubes [24]; and alcohol plus cART group (A+cART), which received both alcohol and cART daily. The animals were treated for 90 days, after which they were weighed, anesthetized with 240 mg/mL pentobarbitone, and terminated. The blood was withdrawn through a cardiac puncture into a plain vacutainer. Thereafter, animals were perfused with 2 mL/min of 0.1 M phosphate buffer in 0.9% saline before extracting the testes. The testes were then preserved for subsequent processing in 10% neutral buffered formalin. Collected blood samples were left to clot and then centrifuged, and the serum was transferred into a new Eppendorf tube for storage at -80°C before analysis.

2.5. Gonadosomatic Index. Final body and testis weights were used to calculate the gonadosomatic index, using the formula previously reported by Olasile et al. [25].

$$\text{Gonadosomatic index} = \frac{\text{Testis weight}}{\text{Body weight}} \times 100(\%). \quad (1)$$

2.6. Immunoassay. Serum levels of reproductive hormones were quantified using enzyme-linked immunosorbent assay (ELISA). A sandwich ELISA technique was used for luteinizing hormone (LH), follicle-stimulating hormone (FSH), and inhibin B, while a competitive ELISA technique was used for testosterone (TT) assay. Before commencing the procedure, serum samples and all reagents were allowed to reach room temperature. Then, the wash buffer, standard working solutions, biotinylated detection antibody, and horseradish peroxidase conjugate were prepared for the assay according to the manufacturer's guidelines. A threefold sample dilution was used for the assay, and standard and samples were run in duplicates (side by side). The assay procedure was carried out as follows. In the case of sandwich (i.e., LH, FSH, and inhibin B), a volume of 100 μL for the standards and samples was carefully added to the bottom of the respective plate wells. Then, the plates were sealed and incubated at 37°C for 90 min. After that, the solution was decanted from the wells, and without washing the plate, 100 μL of the biotinylated detection antibody working solution was added to each well. Afterward, the plate was sealed and incubated at 37°C for 60 min. In the competitive technique for TT assay, a volume of 50 μL for standards and samples was carefully added to the bottom of

the respective plate wells, and immediately, 50 μL of biotinylated detection antibody working solution was added to each well. Subsequently, the plate was sealed and incubated at 37°C for 45 min. Thereafter, the subsequent steps were similar for both techniques. After incubation, the solution was decanted from the wells before three-cycle washing step. The plate was placed in a microplate washer, and 350 μL of wash buffer was added to each well and allowed to soak for 60 sec per cycle. Subsequently, 100 μL of horseradish peroxidase conjugate working solution was added to each well, and the plate was sealed and incubated at 37°C for 30 min. Then, the solution was decanted from the wells, and the wash step was conducted as above for five cycles. Next, 90 μL of substrate reagent was added to each well, and the plate was sealed, wrapped in aluminum foil (to protect it from light), and gently shaken before incubation at 37°C for 15 min, followed by immediate addition of the stop solution to each well of the plate. The plate was put on a microplate reader set at 450 nm filter to measure the optical densities (OD). The microplate reader was set up according to the user's manual guidelines and preheated for 15 minutes before measuring the optical densities. The average OD values for standards and samples were calculated. Then, the average OD for standard zero was subtracted from the average OD for standards and samples. A standard curve was plotted with the standard concentration and OD values. The average OD values for each sample (y-axis) were used to determine the corresponding concentration of TT, LH, FSH, and inhibin B from the standard curve (x-axis). The exact concentration was obtained by multiplying the concentration read of the standard curve with the sample dilution factor.

2.7. Histomorphometric Analyses

2.7.1. Special Histology Stains for Testicular Connective Tissue. The fixed testis tissue was dehydrated in a series of 70-100% alcohol grades and embedded in molten paraffin wax, and sections of 5 μm thickness were cut. Testicular tissue sections were stained with periodic acid Schiff (PAS) (for basement membrane), Masson's trichrome (for capsule and collagen), Gordon and Sweet's silver impregnation (for reticulin), and Gomori's aldehyde fuchsin (for elastin). Stained testis sections were examined using the Axioskop 2 plus light microscope (Nikon Eclipse Ci, 104C type) and photomicrographs captured with the linked computerized Zeiss digital image system, the AxioCam 208 color (Zeiss group, Oberkochen, Germany) for quantification.

2.7.2. Measurement of Seminiferous Tubule Basement Membrane (STBM). Photomicrographs of PAS-stained sections were captured at ×400, and Fiji software was used to measure the thickness of the basement membrane. The thickness of STBM was measured at two points in 50 randomly selected tubules (i.e., 300 tubules per group) [26].

2.7.3. Evaluation of Testicular Capsule Thickness. The capsule thickness was measured on Masson's trichrome-stained sections using Fiji software. Photomicrographs of six fields from the free surface of the capsule were captured at ×400, and three points were measured on each field (i.e., 18 measurements for each animal, 108 per group) [27].

2.7.4. Interstitial Connective Tissue Quantification. Components of testicular connective tissue, i.e., collagen, reticulin, and elastin fibers, were quantified in photomicrographs of sections stained with Masson's trichrome, Gordon and Sweet's silver impregnation, and Gomori's aldehyde fuchsin techniques, respectively. Collagen, reticulin, and elastin fibers were quantified in 24 microscopic fields captured at ×100 for each animal (i.e., 144 fields per group).

(1) Image Processing for Connective Tissue Quantification. The connective tissue images were segmented using ilastik (v1.3.3; https://www.ilastik.org) and subsequently quantified in Fiji software (v1.52e; https://imagej.net/Fiji). Figure 1 illustrates the image processing procedure.

(2) Image Segmentation. The image was divided into fibers and background using the Ilastik pixel classification technique [28, 29]. Briefly, eight sample photos were used to train pixel classifiers (two images per animal group). The classification algorithms included the available features, such as intensity/color, texture, and edge at a sigma of 0.3–10 pixels. Collagen, reticulin, and elastin were appropriately annotated in a few spots of the image (yellow color) to train the classifier. The background, which represents spaces that are not covered by fibers, was then annotated (blue color) (Figure 1). The predictions were inspected after adding each annotation, and the photos were zoomed out to allow more precise placement of annotations. All training photos were then given annotations to improve the classifier and make it more applicable to huge image sets. Once the prediction was of a good standard across the sample images, the trained classifier was applied to training naïve images, and their simple segmentations were exported for quantification.

(3) Image Quantification. The ilastik plugin was used to import the produced image segments from ilastik into Fiji so that they could be quantified into numbers for statistical analysis (Figure 1) [29, 30]. The Fiji scale was modified in accordance with the image's magnification. Area, integrated density, and area fraction were chosen as the measurement parameters and were restricted to the threshold. The connective tissue fibers were then quantified in a macro mode (see Supplementary material (available here)). The percentage area occupied by the connective tissue fibers (collagen, reticulin, and elastin) was calculated as follows:

$$\%\text{Area} = \frac{\text{area of connective fiber}}{\text{total area of photomicrograph}} \times 100. \quad (2)$$

2.8. Immunohistochemistry (IHC) for Androgen Receptor and Ki-67. Testicular tissue sections of 5 μm thickness were mounted onto saline-coated slides and immunolabeled with androgen receptor and Ki-67 antibodies. For antigen retrieval, the sections were treated in citrate buffer pH 6 overnight in a water bath at 60°C. The endogenous peroxidase was then blocked for 20 minutes with 1% hydrogen peroxide in methanol. The sections were then rinsed in phosphate-buffered saline (PBS) before being treated with 5% normal goat serum

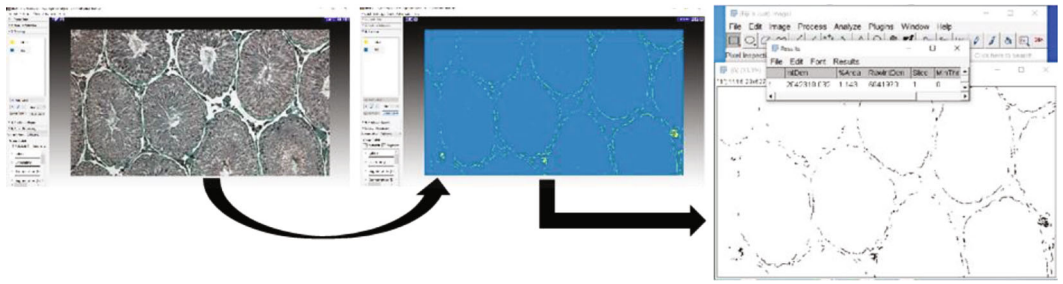

(A) Collagen raw image (B) Segmentation preview (C) Segment quantification

(a)

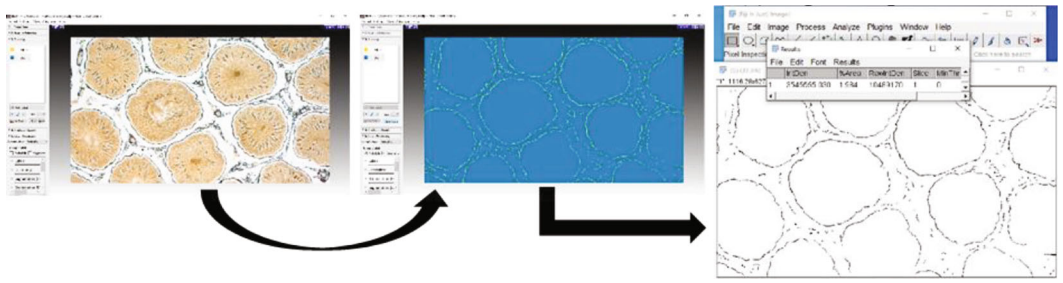

(A) Reticulin raw image (B) Segmentation preview (C) Segment quantification

(b)

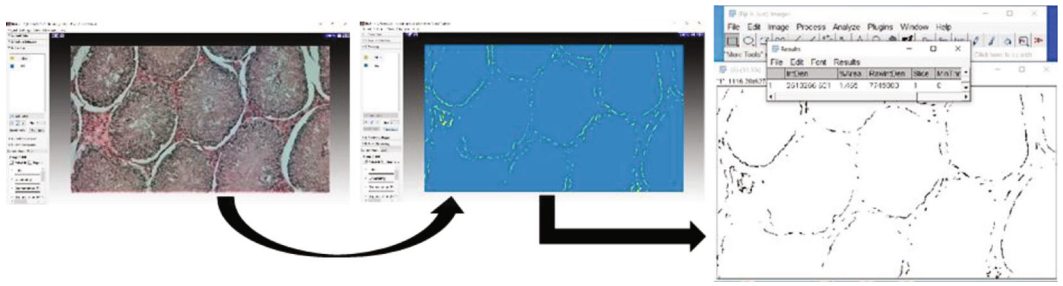

(A) Elastin raw image (B) Segmentation preview (C) Segment quantification

(c)

Figure 1: (a–c) Representative connective tissue image segmentation and quantification in ilastik and Fiji, respectively. The fibers for collagen, reticulin, and elastin were stained using Masson's trichrome, Gordon and Sweet's silver impregnation, and Gomori's aldehyde fuchsin staining technique, respectively. In (a), A, B, and C, respectively, show raw images of collagen, reticulin, and elastin open in ilastik. Preview of image segmented into fibers and background after adding annotations are demonstrated in A, B, and C of (b). The respective exported image segments opened in Fiji displaying quantified respective fibers are shown in A, B, and C of (c).

to prevent nonspecific antibody binding. After 30 minutes, the normal goat serum was tapped off; subsequently, the primary antibody was added (1 : 100 for anti-androgen receptor and 1 : 1000 for anti-Ki-67) and then left at 4°C overnight (approximately 16 hours). Thereafter, the sections were rinsed in PBS and incubated with a 1 : 1000 biotinylated goat anti-rabbit secondary antibody for 30 minutes. Then, after rinsing in PBS, avidin-biotin complex reagent was added for 30 minutes. Afterward, the sections were rinsed in PBS and incubated with 3,3′-diaminobenzidine tetrachloride (DAB) for five minutes. DAB was then washed off under running tap water for five minutes, and the slides were immersed in hematoxylin for one minute, followed by five minutes of washing with running tap water and dehydrating in a series of alcohol. Dibutylphthalate polystyrene xylene was put on the section along with the coverslip. For each antibody, two control slides were included: one without the primary and the other without the secondary antibody. The number of Leydig cells expressing androgen receptor immunoreactivity was counted in 20 microscopic fields at ×400 for each animal (i.e., 120 fields for each group). The number of Sertoli cells expressing androgen receptor immunoreactivity and germ cells expressing Ki-67 immunoreactivity was counted in 20 rounded stages II-VII seminiferous tubules [13] for each animal (i.e., 120 tubules per group).

2.9. Data Analysis. Data analysis was done using the Windows version of GraphPad Prism 6, and the results were presented as mean ± SEM. One-way analysis of variance was used to compare the group means, and the Bonferroni post hoc test was performed afterward. A p value of <0.05 was deemed statistically significant.

3. Results

3.1. Gonadosomatic Index. The study results showed that gonadosomatic index was not significantly different across the animal groups (Table 1).

3.2. Reproductive Hormone Levels. An increase in serum levels of luteinizing and follicle-stimulating hormones was observed in all the treated groups compared to the control (Table 1). The luteinizing hormone level in the A and A +cART groups significantly increased compared to control ($p = 0.0072$ and $p = 0.0027$, respectively). Further, the luteinizing hormone level in the A+cART group increased significantly ($p = 0.0043$) compared to cART, while follicle-stimulating hormone significantly increased in all the treated groups (A, cART, and A+cART) compared to control ($p = 0.0043$, $p = 0.0200$, and $p = 0.0266$, respectively). In comparison with the control group, the decrease in serum levels of testosterone and the difference in inhibin B levels of all the treated groups were insignificant ($p > 0.05$).

3.3. Seminiferous Tubule Basement Membrane (STBM) Thickness. The basement membrane surrounding the seminiferous tubule was identified as a thin periodic acid Schiff-(PAS-) positive staining sheet-like structure with a single layer of flat elongated cells, the myoid cells (Figure 2). Further, positive PAS staining was as well observed in elongated spermatids and some Leydig cells. The testis of animals from the control showed a smooth contoured basement membrane, while the basement membrane of animals treated with alcohol, cART, and A+cART was slightly wavy. The STBM thickness was significantly increased ($p < 0.0001$) in cART-treated animals compared to the control and treated groups A and A+cART (Figure 2). In the A- and A+cART-treated groups, the STBM thickness reduced nonsignificantly when compared to the control group.

3.4. Capsule Thickness. The testicular capsule also referred to as the tunica albuginea comprised of majorly collagen fibers braced with a network of myoid cells (Figure 2). Thickness of the capsule was increased across all the treated groups compared to the control, but a significant increase ($p = 0.0001$) was only recorded in the testis of the A +cART-treated group. Further, capsule thickness of the A +cART-treated group was significantly increased compared to the alcohol and cART groups, $p = 0.0023$ and $p = 0.0064$, respectively (Figure 2).

3.5. Interstitial Connective Tissue. The interstitial connective tissue found between seminiferous tubules and surrounding the tubules consisted of collagen, reticulin, and elastin fibers (Figure 3). A general decrease was recorded in connective tissue components of the treated groups relative to the control group. Collagen content in the treated groups A, cART, and A+cART significantly reduced relative to control, $p = 0.0176$, $p < 0.0001$, and $p < 0.0001$, respectively. Further, collagen in the cART group was significantly decreased compared to A ($p < 0.0001$) and A+cART ($p = 0.0225$). A significant reduction in reticulin fibers was found in the cART- and A+cART-treated groups compared to control ($p = 0.0154$ and $p < 0.0001$, respectively), while reticulin of the A+cART group was significantly reduced compared to the A ($p < 0.0001$) and cART ($p = 0.0004$) treated groups. In comparison with the control group, elastin was significantly reduced in all the treated groups (A: $p = 0.0144$, cART: $p = 0.0338$, and A+cART: $p = 0.0010$) (Figure 3).

3.6. Immunohistochemistry for Androgen Receptor and Germ Cell Proliferation (Ki-67)

3.6.1. Androgen Receptor. In all groups, nuclei of Sertoli, Leydig, pericyte, and myoid cells were positively immunostained with androgen receptor antibody (Figure 4). Noteworthy, germ cells did not show positive immunostaining for androgen receptor either in their cytoplasm or nucleus. The number of Sertoli cells expressing androgen receptor significantly decreased in the cART- and A +cART-treated groups compared to control ($p < 0.0001$) and A ($p = 0.0025$ and $p < 0.0001$, respectively). Further, the number of Sertoli cells expressing androgen receptor in the A+cART group decreased significantly compared to cART ($p = 0.0195$). But the number of Leydig cells expressing androgen receptor reduced significantly in all the treated groups compared to the control (A: $p = 0.0438$, cART: $p < 0.0001$, and A+cART: $p < 0.0001$). In addition, Leydig cells expressing androgen receptor in the cART- and A+cART-treated groups decreased significantly compared to A ($p = 0.0164$ and $p < 0.0001$). However, the number of Leydig cells expressing androgen receptor in A+cART was significantly decreased compared to cART ($p = 0.0007$) (Figure 4).

3.6.2. Germ Cell Proliferation (Ki-67). Proliferation marker Ki-67 was expressed mainly in spermatocytes and round spermatids across the animal groups. The number of germ cells expressing Ki-67 reduced significantly in all the treated groups compared to the control group (A: $p = 0.0129$, cART: $p = 0.0046$, and A+cART: $p = 0.0002$) (Figure 5).

4. Discussion

The processes involved in testis development, spermatogenesis, and steroidogenesis are tightly regulated by the hypothalamic-pituitary-gonadal (HPG) axis hormones, i.e., luteinizing hormone (LH), follicle-stimulating hormone (FSH), and testosterone (TT) [12, 31]. These hormones work via respective receptors present in the testicular somatic cells and are controlled through a negative feedback mechanism [9, 32]. The LH and FSH receptors are exclusively present in the Leydig and Sertoli cells, respectively [31, 33], while the TT receptors also known as the androgen receptors (AR) are expressed by Leydig, Sertoli, myoid, and pericyte cells [19, 20]. Though changes in levels of reproductive hormones have been studied extensively in several male reproductive dysfunctions, investigations about the changes in their respective receptors are scanty. Nevertheless, reproductive hormone receptor resistance, receptor reduction, or both, including changes in reproductive hormone levels, are major contributing factors for male reproductive dysfunctions and infertility [12, 15].

Table 1: Mean gonadosomatic index and serum levels of reproductive hormones for rats treated with alcohol, cART, and both.

Animal groups	Control	Alcohol (A)	cART	A+cART
Gonadosomatic index (%)	0.37 ± 0.03	0.37 ± 0.02	0.36 ± 0.03	0.38 ± 0.02
Reproductive hormones				
Luteinizing hormone (mIU/mL)	67.23 ± 8.98	109.9 ± 9.76[a]	82.16 ± 5.38	112.9 ± 4.03[ab]
Follicle-stimulating hormone (ng/mL)	69.94 ± 8.80	129 ± 5.26[a]	127.2 ± 16.52[a]	118.2 ± 12.09[a]
Testosterone (ng/mL)	2.83 ± 0.46	2.66 ± 0.49	2.19 ± 0.59	2.14 ± 0.04
Inhibin B (pg/mL)	72.74 ± 6.23	71.78 ± 3.92	74.67 ± 1.69	69.16 ± 4.74

[a]Significant compared to the control group in the same row. [b]Significant compared to the cART group in the same row. Gonadosomatic index was not significantly ($p > 0.05$) different across the groups. Luteinizing hormone of the cART and A+cART groups increased significantly ($p < 0.05$) compared to A, and A+cART was significantly increased compared to cART. Follicle-stimulating hormone of the cART and A+cART groups significantly increased ($p < 0.05$) compared to control. No statistical difference was found in testosterone and inhibin B levels across the animal groups.

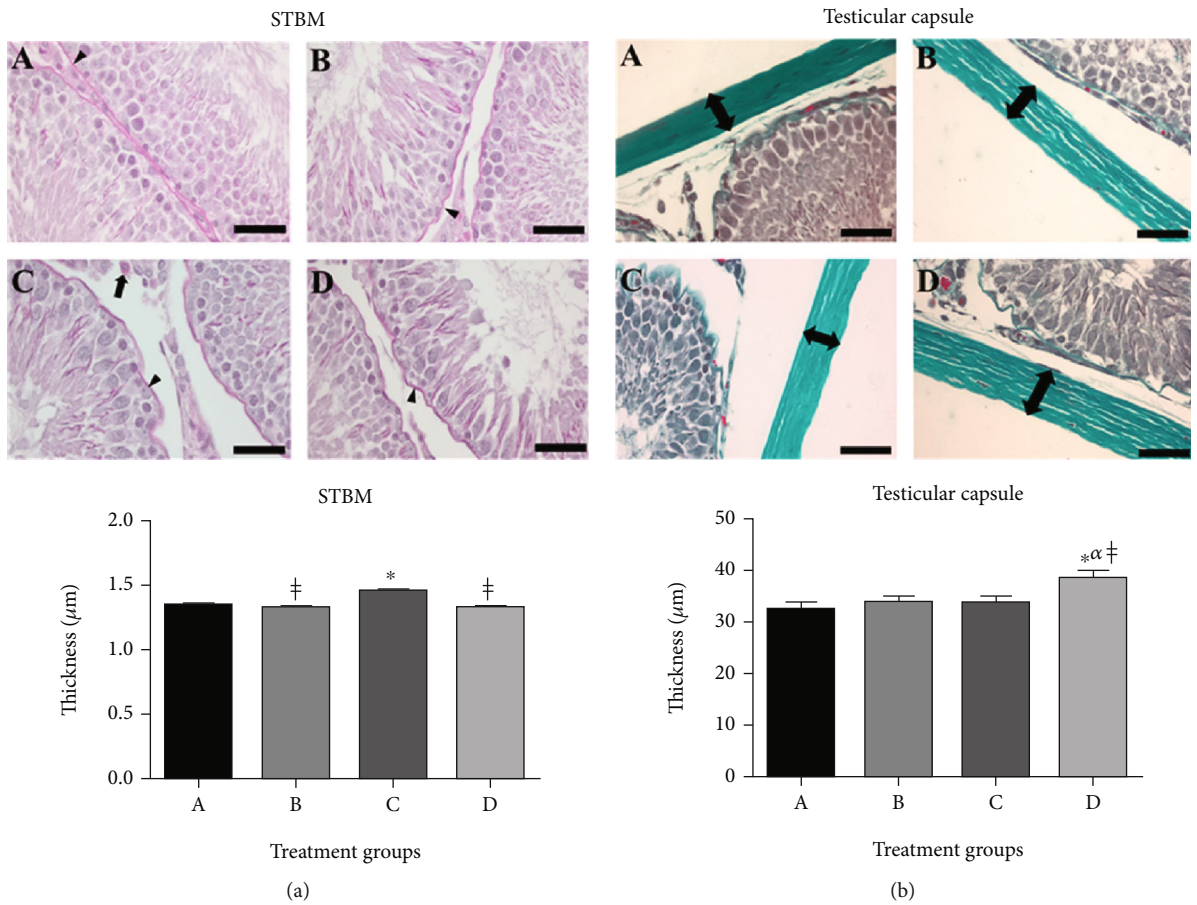

Figure 2: (a) Representative seminiferous tubule basement membrane (STBM) (arrowheads) and testicular capsule (double arrows) photomicrographs, PAS and Masson's Trichrome stain, respectively. (b) Leydig cell PAS positive (thick arrow) shown in a cART photomicrograph. Graphs show respective mean thickness. Different symbols *, α, and ‡ represent comparison with groups control, alcohol, and cART, respectively. STBM thickness in cART increased significantly ($p < 0.05$) compared to groups control, alcohol, and A +cART. Capsule thickness in A+cART was significantly increased ($p < 0.05$) compared to control and cART. Magnification, ×400; scale bar, 50 μm. Key: image: A, control group; B, alcohol group; C, cART group, and D, A+cART group.

In this study, we observed a significantly elevated LH levels in the alcohol- and A+cART-treated groups and FSH in all the treated groups, but no significant changes were detected in levels of TT and inhibin B relative to control. Similar results of enhanced LH and FSH levels with serious adverse impacts on reproductive male parameters have been reported following alcohol abuse [34]. Furthermore, decreased or normal TT levels together with elevated gonadotropins (LH and FSH) levels, similar to the present result, are associated with poor sperm quality and azoospermia [35]. However, contrary to our findings, a previous report [9] indicated a reduction in LH, FSH, and TT levels in rats

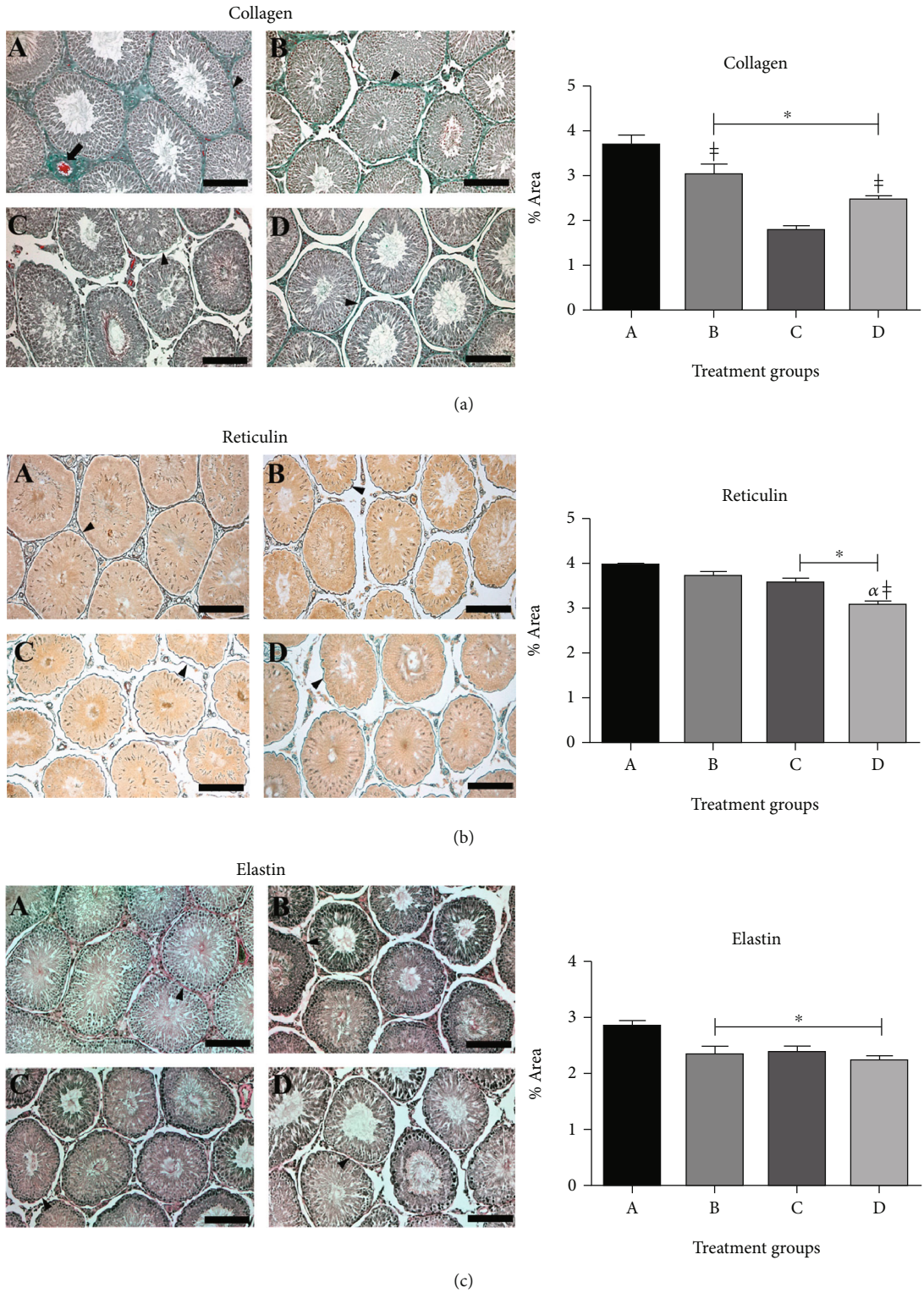

Figure 3: (a–c) Representative collagen, reticulin, and elastin indicated with arrowheads in photomicrographs, Masson's trichrome, Gordon and Sweet's silver impregnation, and Gomori's aldehyde fuchsin stain, respectively. A thick arrow indicating a blood vessel is shown in the collagen photomicrograph, A. Graphs show respective mean percentage areas. Different symbols *, α, and ǂ represent comparison with groups control, alcohol, and cART, respectively. Collagen of the alcohol, cART, and A+cART groups decreased significantly ($p < 0.05$) compared to control, while collagen in cART was significantly decreased compared to alcohol and A+cART. Reticulin significantly decreased ($p < 0.05$) in the cART and A+cART groups compared to control; further, reticulin in A+cART decreased significantly compared to A and cART. Elastin in the alcohol-, cART-, and A+cART-treated groups was significantly decreased ($p < 0.05$) compared to control. Magnification, ×100; scale bar, 200 μm. Key: image: A, control group; B, alcohol group; C, cART group; and D, A+cART group.

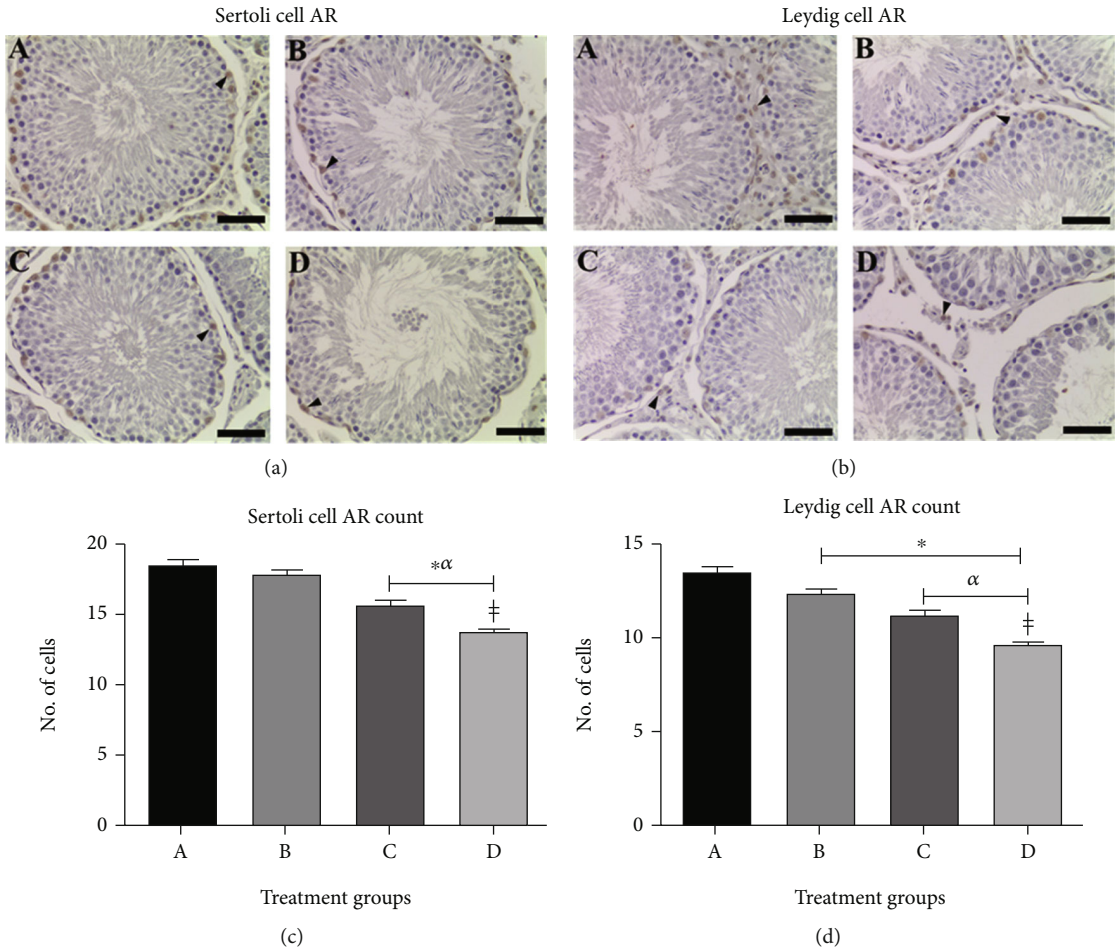

Figure 4: (a, b) Representative photomicrographs showing Sertoli and Leydig cell androgen receptor (AR) immunoreactivity (arrowheads) and respective mean number of immunoreactive cell graphs. Different symbols *, α, and ‡ represent comparison with groups control, alcohol (A), and cART, respectively. (c) Sertoli cell AR count decreased significantly ($p < 0.05$) in the cART and A+cART groups compared to control and A; further, A+cART was significantly decreased compared to cART. (d) Leydig cell AR count of the A, cART, and A+cART groups significantly decreased ($p < 0.05$) compared to control, while cART and A+cART were decreased significantly compared to the A-treated group, and Leydig cell AR count was significantly decreased in the A+cART group when compared to the cART group. Magnification, ×400; scale bar, 50 μm. Key: image: A, control group; B, alcohol group; C, cART group; and D, A+cART group.

treated with alcohol. Discrepancies in reports also exist on the impact of cART on reproductive hormones levels, with some studies showing no significant changes [7], decreased levels [36], and increased levels [37, 38]. In this study, animals treated with cART had significantly increased FSH levels, an insignificant increase in LH and inhibin B levels, but TT level was insignificantly decreased. The conflicting results could be due to the different doses and durations of the treatments and the different drug component combinations in the case of cART studies.

Notably, normal germ cell development requires a well-balanced interplay between reproductive hormones of the HPG axis, gonadotropins (LH and FSH), and testicular hormones (TT and inhibin B) [12]. Consequently, alteration in the negative feedback mechanism signals would lead to hormonal imbalance and subsequently affect the processes and progress of spermatogenesis [32]. The negative feedback mechanism for gonadotropin-releasing hormone (GnRH) and LH production by the hypothalamus and pituitary, respectively, is modulated by TT [12, 31]. Inhibin B, a gonadal peptide hormone synthesized by Sertoli cells, is responsible for the FSH feedback regulation [15, 32]. Therefore, the observed significant elevations of LH and FSH with unaltered TT and inhibin B levels in treated animals could have resulted from a disruption in the feedback mechanism, which invariably will lead to dysregulation of spermatogenesis. Additionally, the hormonal imbalance might result from a hormone-receptor resistant state due to a decrease in androgen receptors and/or sensitivity, which is characterized by elevated LH levels and normal or increased TT [12, 39].

Since germ cells do not express androgen receptors, the impact of TT on spermatogenesis is mediated via Sertoli cells' androgen receptors [14, 15, 22]. We found a significant decrease in the number of Sertoli cells expressing androgen receptors in the testis of animals treated with cART and A +cART. This implies a dysfunction of androgen receptors, which subsequently leads to spermatogenesis failure. Also, previous studies have linked depletion of androgen receptors

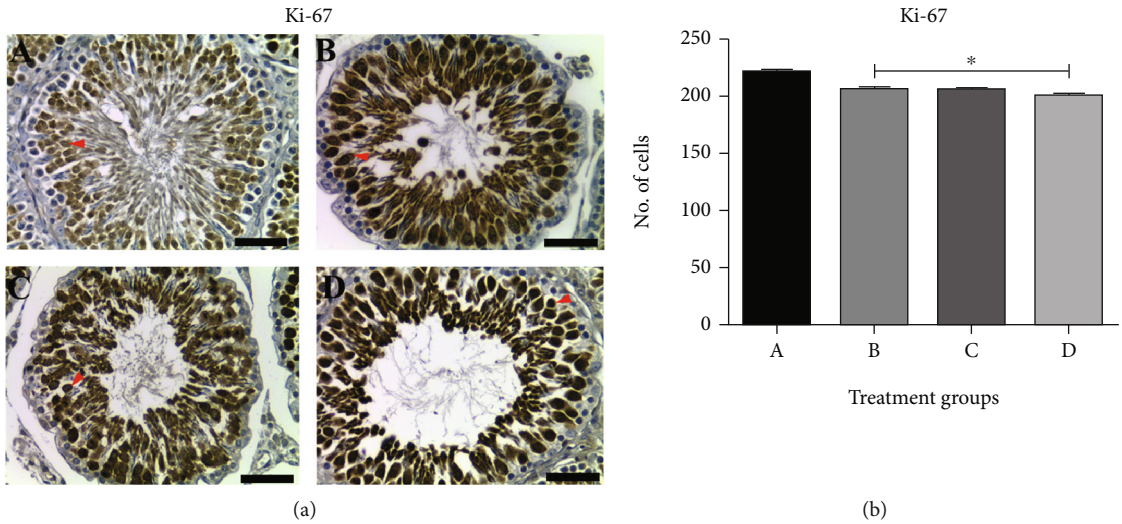

FIGURE 5: (a, b) Representative photomicrographs showing Ki-67 immunoreactivity (arrowheads) and a graph of the mean number of immunoreactive cells. Different symbols *, α, and ǂ represent comparison with groups control, alcohol (A), and cART, respectively. The expression of Ki-67 was significantly reduced ($p < 0.05$) in the A-, cART-, and A+cART-treated groups compared to control. Magnification, ×400; scale bar, 50 μm. Key: image: A, control group; B, alcohol group; C, cART group; and D, A+cART group.

to male infertility [14] and increased risk of germ cell malignancy [40]. Although the expression of androgen receptors following alcohol or/and cART has not been widely reported, one study found a weak androgen receptor expression in the testis of animals treated with cART [41]. Other toxic chemicals such as organochlorinated pesticides, industrial chemicals, and plasticizers have been shown to diminish the number and action of androgen receptors [42]. A study by Qiu et al. [43] reported significantly decreased androgen receptor expression in the testis of rats exposed to bisphenol A. Further, in vivo studies in male mice have demonstrated testicular feminizing syndrome (characterized by microphallus penis, urethral hypospadias, small undescended testes, labia majora-like scrotal sac, and absence of vas deferens, epididymis, seminal vesicle, and prostate) following androgen receptor knockout [17, 44].

Conversely, a reduction in androgen receptors points to a disruption in the regulatory activity of testosterone on spermatogenesis. However, a nonsignificant decrease in the number of Sertoli cells expressing AR recorded in the testis of animals treated with only alcohol could be the underlying mechanism for the restoration of testicular function when alcohol abuse is discontinued. Previous human and animal studies have reported restoration of normal spermatogenesis after abstaining from alcohol [45, 46]. Furthermore, androgen receptors regulate the function and structure of the cells such as Leydig, Sertoli, myoid, and pericyte cells, which are involved in the regulation of spermatogenic process [17–19].

Remarkably, androgen receptor expression modulates Sertoli and myoid cell secretory function [47, 48], including secretion of components of connective tissue and tubule basement membrane such as collagen and laminin [15, 18]. We observed a general increase in testicular capsule and seminiferous tubule basement membrane thickness of the treated groups compared to the control, but a significant increase in these parameters was only recorded in A+cART- and cART-treated animals, respectively. Such increases may suggest structural alterations induced by treatments, which will lead to capsular and seminiferous tubule basement membrane dysfunctions [25, 49]. These changes complement the decrease in the components of connective tissue (collagen, reticulin, and elastin) recorded in the testis of all treated animals. Conversely, earlier studies demonstrated elevated collagenase enzyme activity following exposure to alcohol [50] and cART [51], which causes fibroblast dysfunction and increased connective tissue fiber degradation and consequently leads to a reduction in connective tissue deposit [50, 51]. In addition, Ranzer et al. [52] found that decreased fibroblast proliferative activity and type 1 collagen synthesis capacity led to a reduction of collagen content following alcohol exposure. However, due to a shared cytochrome P450 metabolic pathway, the interaction between the treatment chemicals (alcohol and cART) could mildly diminish some of their independent impacts as reflected by the lesser decrease in collagen content in the testis of animals treated with both alcohol and cART (A+cART group).

Consistent with our findings, earlier studies reported deleterious effects of alcohol [53] and cART [54] on the testicular capsule. Studies by Ogedengbe et al. [49] and Olasile et al. [25] found distorted and thickened seminiferous tubule basement membrane in cART-treated animals. Further, changes in collagen [55] and absence of reticulin fibers [56] have been demonstrated in rats exposed to alcohol. Testicular connective tissue, including the capsule, interstitial tissue, and seminiferous tubule basement membrane play a crucial role in maintaining testicular structural integrity and functioning and also enable spermatozoa propulsive movement to the rete testis [27, 57]. This is a crucial function in the reproductive process and is attributed to the contractility of myoid cells [48, 57]. Conversely, the alterations recorded in these parameters in the treated groups suggest testicular toxicity and spermatogenesis failure.

Associated with the normal physiology and integrity of the testicular structure is the constant cell division and germ cell proliferation for continuous sperm production. Thus, the germ cells at different stages of spermatogenesis express a nucleus-associated proliferation marker, the Ki-67 [58] that regulates the cell cycle and chromosomal structure and integrity [59]. Consistent with previous reports on testicular toxicity [58, 60], a significant decrease in the number of germ cells expressing Ki-67 was recorded in all the treated groups relative to control. This suggests impaired testicular germ cell proliferation which ultimately translates to diminished spermatozoa production.

5. Conclusions

This study demonstrated that exposure to alcohol, combination antiretroviral therapy (cART), or both disrupts the HPG axis function and testis structure integrity, leading to testicular dysfunction. The treated animal groups showed alteration in reproductive hormone levels, seminiferous tubule basement membrane and testicular capsule thickness, interstitial connective tissue fibers (collagen, reticulin, and elastin), and Sertoli and Leydig cell androgen receptor and germ cell Ki-67 expression. With exception of seminiferous tubule basement membrane thickness, all the observed changes were exacerbated in the animals treated with both alcohol and cART (A+cART group), implying a severe impact of alcohol and cART concurrent use on the male reproductive function. Further, our findings suggest that depletion of androgen receptors might be an underlying mechanism for inducing testis structure and spermatogenesis impairments by chemical insults (alcohol or/and cART). Therefore, the study results may be clinically invaluable in the management of male sexual insufficiency and reproductive failure, especially in HIV/AIDS-positive individuals on cART regimen and who drink alcohol regularly.

Data Availability

The datasets for the results reported in this study will be made available through a University of the Witwatersrand archived link.

Conflicts of Interest

The authors declare no conflicts of interest.

Acknowledgments

We appreciate the collaborative efforts of our colleagues Jaclyn Asouzu Johnson, Idemudia Eguavoen, and Vaughan Perry and extend special appreciation to Hasiena Ali for her laboratory assistance. This research was funded partly by Professor Mbajiorgu's Wits Faculty of Health Sciences Research Publication Incentive (RINC) grant (grant number: 001.167.8421101.5122201/4228) and supplemented by the Wits School of Anatomical Sciences Research grant (grant number: 001.251.8421101.5122201/4708). Open access funding is enabled and organized by the SANLiC Gold.

Supplementary Materials

Macro script for connective tissue fiber quantification. *(Supplementary Materials)*

References

[1] T. Khawcharoenporn and B. E. Sha, *HIV infection and infertility*, IntechOpen, 2016.

[2] WHO, *Global Status Report on Alcohol and Health 2018: Executive Summary*, World Heal, Organ, 2018.

[3] S. A. Lippman, A. M. El Ayadi, J. S. Grignon et al., "Improvements in the South African HIV care cascade: findings on 90-90-90 targets from successive population-representative surveys in North West Province," *Journal of the International AIDS Society*, vol. 22, no. 6, p. e25295, 2019.

[4] UNAIDS, *UNAIDS Fact Sheet*, Glob. HIV Stat., 2021.

[5] H. M. Crane, M. E. McCaul, G. Chander et al., "Prevalence and factors associated with hazardous alcohol use among persons living with HIV across the US in the current era of antiretroviral treatment," *AIDS and Behavior*, vol. 21, no. 7, pp. 1914–1925, 2017.

[6] M. Necho, A. Belete, and Y. Getachew, "The prevalence and factors associated with alcohol use disorder among people living with HIV/AIDS in Africa: a systematic review and meta-analysis," *Substance Abuse Treatment, Prevention, and Policy*, vol. 15, no. 1, p. 63, 2020.

[7] O. O. Ogedengbe, E. C. S. Naidu, E. N. Akang et al., "Virgin coconut oil extract mitigates testicular-induced toxicity of alcohol use in antiretroviral therapy," *Andrology*, vol. 6, no. 4, pp. 616–626, 2018.

[8] O. O. Ogedengbe, E. C. S. Naidu, and O. O. Azu, "Antiretroviral therapy and alcohol interactions: X-raying testicular and seminal parameters under the HAART era," *European Journal of Drug Metabolism and Pharmacokinetics*, vol. 43, no. 2, pp. 121–135, 2018.

[9] A. A. Oremosu and E. N. Akang, "Impact of alcohol on male reproductive hormones, oxidative stress and semen parameters in Sprague-Dawley rats," *Middle East Fertility Society Journal*, vol. 20, no. 2, pp. 114–118, 2015.

[10] N. Wong, M. Levy, and I. Stephenson, "Hypogonadism in the HIV-infected man," *Current Treatment Options in Infectious Diseases*, vol. 9, no. 1, pp. 104–116, 2017.

[11] Y. Duca, A. Aversa, R. A. Condorelli, A. E. Calogero, and S. La Vignera, "Substance abuse and male hypogonadism," *Journal of Clinical Medicine*, vol. 8, no. 5, p. 732, 2019.

[12] P. F. Corradi, R. B. Corradi, and L. W. Greene, "Physiology of the hypothalamic pituitary gonadal axis in the male," *The Urologic Clinics of North America*, vol. 43, no. 2, pp. 151–162, 2016.

[13] W. J. Bremner, M. R. Millar, R. M. Sharpe, and P. T. K. Saunders, "Immunohistochemical localization of androgen receptors in the rat testis: evidence for stage-dependent expression and regulation by androgens," *Endocrinology*, vol. 135, no. 3, pp. 1227–1234, 1994.

[14] L. O'Hara and L. B. Smith, "Androgen receptor roles in spermatogenesis and infertility," *Best Practice & Research. Clinical Endocrinology & Metabolism*, vol. 29, no. 4, pp. 595–605, 2015.

[15] C. Petersen and O. Söder, "The Sertoli cell - a hormonal target and "super" nurse for germ cells that determines testicular size," *Hormone Research*, vol. 66, no. 4, pp. 153–161, 2006.

[16] W. Shah, R. Khan, B. Shah et al., "The molecular mechanism of sex hormones on Sertoli cell development and proliferation," *Frontiers in Endocrinology*, vol. 12, 2021.

[17] R. S. Wang, S. Yeh, C. R. Tzeng, and C. Chang, "Androgen receptor roles in spermatogenesis and fertility: lessons from testicular cell-specific androgen receptor knockout mice," *Endocrine Reviews*, vol. 30, no. 2, pp. 119–132, 2009.

[18] C. Mayer, M. Adam, L. Walenta et al., "Insights into the role of androgen receptor in human testicular peritubular cells," *Andrology*, vol. 6, no. 5, pp. 756–765, 2018.

[19] L. X. Shan, C. W. Bardin, and M. P. Hardy, "Immunohistochemical analysis of androgen effects on androgen receptor expression in developing Leydig and Sertoli cells," *Endocrinology*, vol. 138, no. 3, pp. 1259–1266, 1997.

[20] M. Basiri, M. Asadi-Shekaari, M. Ezzatabdipour, A. Sarv Azad, and S. N. Nematollahimahani, "Immunohistochemistry study on androgen and estrogen receptors of rat seminal vesicle submitted to simultaneous alcohol-nicotine treatment," *Cell Journal (Yakhteh)*, vol. 18, no. 3, pp. 458–463, 2016.

[21] G. Kaur, L. A. Thompson, and J. M. Dufour, "Sertoli cells - immunological sentinels of spermatogenesis," *Seminars in Cell & Developmental Biology*, vol. 30, pp. 36–44, 2014.

[22] L. B. Smith and W. H. Walker, "The regulation of spermatogenesis by androgens," *Seminars in Cell & Developmental Biology*, vol. 30, pp. 2–13, 2014.

[23] G. Dutra Gonçalves, N. Antunes Vieira, H. Rodrigues Vieira et al., "Role of resistance physical exercise in preventing testicular damage caused by chronic ethanol consumption in UChB rats," *Microscopy Research and Technique*, vol. 80, no. 4, pp. 378–386, 2017.

[24] R. E. Akhigbe, M. A. Hamed, and A. O. Aremu, "HAART exacerbates testicular damage and impaired spermatogenesis in anti-Koch-treated rats via dysregulation of lactate transport and glutathione content," *Reproductive Toxicology*, vol. 103, pp. 96–107, 2021.

[25] I. O. Olasile, I. Ayoola Jegede, O. Ugochukwu et al., "Histomorphological and seminal evaluation of testicular parameters in diabetic rats under antiretroviral therapy: interactions with hypoxis hemerocallidea," *Iranian Journal of Basic Medical Sciences*, vol. 21, pp. 1316–1324, 2018.

[26] S. S. Omar, R. G. Aly, and N. M. Badae, "Vitamin E improves testicular damage in streptozocin-induced diabetic rats, via increasing vascular endothelial growth factor and poly(ADP-ribose) polymerase-1," *Andrologia*, vol. 50, no. 3, article e12925, 2018.

[27] T. A. Aire and P. C. Ozegbe, "The testicular capsule and peritubular tissue of birds: morphometry, histology, ultrastructure and immunohistochemistry," *Journal of Anatomy*, vol. 210, no. 6, pp. 731–740, 2007.

[28] S. Berg, D. Kutra, T. Kroeger et al., "Ilastik: interactive machine learning for (bio)image analysis," *Nature Methods*, vol. 16, no. 12, pp. 1226–1232, 2019.

[29] Y. H. Chim, H. A. Davies, D. Mason et al., "Bicuspid valve aortopathy is associated with distinct patterns of matrix degradation," *The Journal of Thoracic and Cardiovascular Surgery*, vol. 160, no. 6, pp. e239–e257, 2020.

[30] H. A. Lucero, S. Patterson, S. Matsuura, and K. Ravid, "Quantitative histological image analyses of reticulin fibers in a myelofibrotic mouse," *Journal of Biological Methods*, vol. 3, no. 4, p. e60, 2016.

[31] P. Marques, K. Skorupskaite, J. T. George, and R. A. Anderson, "Physiology of GNRH and Gonadotropin Secretion," *Endotext*, 2000, http://www.ncbi.nlm.nih.gov/pubmed/25905297.

[32] R. I. Clavijo and W. Hsiao, "Update on male reproductive endocrinology," *Translational Andrology and Urology*, vol. 7, pp. S367–S372, 2018.

[33] P. Gurung, E. Yetiskul, and I. Jialal, "Physiology, Male Reproductive System," *StatPearls*, 2023, http://www.ncbi.nlm.nih.gov/pubmed/30860700.

[34] K. R. Muthusami and P. Chinnaswamy, "Effect of chronic alcoholism on male fertility hormones and semen quality," *Fertility and Sterility*, vol. 84, no. 4, pp. 919–924, 2005.

[35] W. Zhao, J. Jing, Y. Shao et al., "Circulating sex hormone levels in relation to male sperm quality," *BMC Urology*, vol. 20, no. 1, p. 101, 2020.

[36] R. E. Akhigbe, M. A. Hamed, and A. F. Odetayo, "HAART and anti-Koch's impair sexual competence, sperm quality and offspring quality when used singly and in combination in male Wistar rats," *Andrologia*, vol. 53, no. 2, p. e13951, 2021.

[37] J. Collazos, E. Martínez, J. Mayo, and S. Ibarra, "Sexual dysfunction in HIV-infected patients treated with highly active antiretroviral therapy," *Journal of Acquired Immune Deficiency Syndromes*, vol. 31, no. 3, pp. 322–326, 2002.

[38] S. O. Olojede, S. K. Lawal, O. S. Faborode et al., "Testicular ultrastructure and hormonal changes following administration of tenofovir disoproxil fumarate-loaded silver nanoparticle in type-2 diabetic rats," *Scientific Reports*, vol. 12, no. 1, p. 9633, 2022.

[39] I. A. Hughes, J. D. Davies, T. I. Bunch, V. Pasterski, K. Mastroyannopoulou, and J. Macdougall, "Androgen insensitivity syndrome," *In The Lancet*, vol. 380, no. 9851, pp. 1419–1428, 2012.

[40] B. A. Barros, L. R. De Oliveira, C. R. C. Surur, A. D. A. Barros-Filho, A. T. Maciel-Guerra, and G. Guerra-Junior, "Complete androgen insensitivity syndrome and risk of gonadal malignancy: systematic review," *Annals of Pediatric Endocrinology & Metabolism*, vol. 26, no. 1, pp. 19–23, 2021.

[41] O. O. Ismail, J. A. Isaac, O. Ugochukwu et al., "Impaired expression of testicular androgen receptor and collagen fibers in the testis of diabetic rats under HAART: the role of Hypoxis hemerocallidea," *Folia Histochemica et Cytobiologica*, vol. 55, no. 3, pp. 149–158, 2017.

[42] D. C. Luccio-Camelo and G. S. Prins, "Disruption of androgen receptor signaling in males by environmental chemicals," *The Journal of Steroid Biochemistry and Molecular Biology*, vol. 127, no. 1-2, pp. 74–82, 2011.

[43] L.-L. Qiu, X. Wang, X. Zhang et al., "Decreased androgen receptor expression may contribute to spermatogenesis failure in rats exposed to low concentration of bisphenol A," *Toxicology Letters*, vol. 219, no. 2, pp. 116–124, 2013.

[44] S. Yeh, M. Y. Tsai, Q. Xu et al., "Generation and characterization of androgen receptor knockout (ARKO) mice: an in vivo model for the study of androgen functions in selective tissues," *Proceedings of the National Academy of Sciences of the United States of America*, vol. 99, no. 21, pp. 13498–13503, 2002.

[45] O. O. Dosumu, A. A. A. Osinubi, and F. I. O. Duru, "Alcohol induced testicular damage: can abstinence equal recovery?," *Middle East Fertility Society Journal*, vol. 19, pp. 221–228, 2014.

[46] B. Guthauser, F. Boitrelle, A. Plat, N. Thiercelin, and F. Vialard, "Chronic excessive alcohol consumption and male fertility: a case report on reversible azoospermia and a

literature review," *Alcohol and Alcoholism*, vol. 49, no. 1, pp. 42–44, 2014.

[47] P. P. Pöllänen, M. Kallajoki, L. Risteli, J. Risteli, and J. J. O. Suominen, "Laminin and type IV collagen in the human testis," *International Journal of Andrology*, vol. 8, no. 5, pp. 337–347, 1985.

[48] A. Mayerhofer, "Human testicular peritubular cells: more than meets the eye," *Reproduction*, vol. 145, no. 5, pp. R107–R116, 2013.

[49] O. O. Ogedengbe, A. I. Jegede, I. O. Onanuga et al., "Coconut oil extract mitigates testicular injury following adjuvant treatment with antiretroviral drugs," *Toxicology Research*, vol. 32, no. 4, pp. 317–325, 2016.

[50] G. Kanbak, M. Canbek, A. Oğlakçı et al., "Preventive role of gallic acid on alcohol dependent and cysteine protease-mediated pancreas injury," *Molecular Biology Reports*, vol. 39, no. 12, pp. 10249–10255, 2012.

[51] L. Hansen, I. Parker, L. M. Roberts, R. L. Sutliff, M. O. Platt, and R. L. Gleason, "Azidothymidine (AZT) leads to arterial stiffening and intima-media thickening in mice," *Journal of Biomechanics*, vol. 46, no. 9, pp. 1540–1547, 2013.

[52] M. J. Ranzer, L. Chen, and L. A. DiPietro, "Fibroblast function and wound breaking strength is impaired by acute ethanol intoxication," *Alcoholism, Clinical and Experimental Research*, vol. 35, no. 1, pp. 83–90, 2011.

[53] I. E. Asuquo, I. A. Edagha, G. J. Ekandem, and A. I. Peter, "Carica papaya attenuates testicular histomorphological and hormonal alterations following alcohol-induced gonado toxicity in male rats," *Toxicology Research*, vol. 36, no. 2, pp. 149–157, 2020.

[54] S. O. Olojede, S. K. Lawal, A. Dare et al., "Highly active antiretroviral therapy conjugated silver nanoparticle ameliorates testicular injury in type-2 diabetic rats," *Heliyon*, vol. 7, no. 12, p. e08580, 2021.

[55] G. M. Shayakhmetova, L. B. Bondarenko, V. M. Kovalenko, and V. V. Ruschak, "CYP2E1 testis expression and alcoholmediated changes of rat spermatogenesis indices and type I collagen," *Archives of Industrial Hygiene and Toxicology*, vol. 64, no. 2, pp. 237–246, 2013.

[56] F. A. Fakoya and E. A. Caxton-Martins, "Morphological alterations in the seminiferous tubules of adult Wistar rats: the effects of prenatal ethanol exposure," *Folia Morphologica*, vol. 63, no. 2, pp. 195–202, 2004.

[57] D. Fleck, L. Kenzler, N. Mundt et al., "ATP activation of peritubular cells drives testicular sperm transport," *eLife*, vol. 10, pp. 1–30, 2021.

[58] W. P. Zhao, H. W. Wang, J. Liu et al., "Positive PCNA and Ki-67 expression in the testis correlates with spermatogenesis dysfunction in fluoride-treated rats," *Biological Trace Element Research*, vol. 186, no. 2, pp. 489–497, 2018.

[59] S. Cuylen-Haering, M. Petrovic, A. Hernandez-Armendariz et al., "Chromosome clustering by Ki-67 excludes cytoplasm during nuclear assembly," *Nature*, vol. 587, no. 7833, pp. 285–290, 2020.

[60] J. H. Moon, D. Y. Yoo, Y. K. Jo et al., "Unilateral chryptochidism induces morphological changes of testes and hyperplasia of Sertoli cells in a dog," *Laboratory Animal Research*, vol. 30, no. 4, pp. 185–189, 2014.